

# Ca<sub>0.85</sub>Sm<sub>0.15</sub>MnO<sub>3</sub>: A mixed antiferromagnet with unusual properties

R. Mahendiran, A. Maignan, C. Martin, M. Hervieu, and B. Raveau

*Laboratoire CRIMAT, ISMRA, Université de Caen, 6. Boulevard du  
Maréchal Juin, Caen Cedex -14050, France*

(November 14, 2018)

## Abstract

We establish a phase diagram for the electron-doped manganites Ca<sub>1-x</sub>Sm<sub>x</sub>MnO<sub>3</sub> ( $0 \leq x \leq 0.15$ ). The low temperature insulating phase of  $x = 0.15$  is a mixed antiferromagnet with two long range antiferromagnetism, C-type (monoclinic) and G-type (orthorhombic), coexisting with short range ferromagnetic clusters (orthorhombic). Resistivity ( $\rho$ ) and magnetization ( $M$ ) of  $x = 0.15$  show unusual magnetic field history dependent phenomena which are not observed for  $x \leq 0.12$ : irreversibility between zero field-cooled (ZFC) and field-cooled (FC) data below 120 K and hysteresis between cooling and warming for all values of magnetic fields ( $0 \leq H \leq 7$  T). Field cooling strongly enhances  $M$  ( $M_{FC}/M_{ZFC} = 2.7$  at  $H = 5$  T and 10K) reduces  $\rho$  ( $\rho_{FC}/\rho_{ZFC} = 1.5 \times 10^{-4}$  at 7 T and 10 K) and even induces metallic-like resistivity ( $d\rho/dT > 0$ ) for  $H = 7$  T below 80 K. We discuss the possible origins of the results.

Coexistence of itinerant and localized charges over different length scales, known as the electronic phase separation, seems to be one of the fundamental aspects of colossal magnetoresistive manganites of the type  $R_{1-x}A_x\text{MnO}_3$  where R and A are trivalent rare earth and divalent alkali ions respectively. The electronic phase separation in manganites also induces magnetic phase separation as the hopping of  $e_g$  hole between  $\text{Mn}^{4+}:t_{2g}^3e_g^0$ -O- $\text{Mn}^{3+}:t_{2g}^3e_g^1$  is facilitated if  $t_{2g}^3$  spins are ferromagnetically aligned and hindered if they are antiferromagnetically aligned. Thus, phase separation manifests itself as isolated ferromagnetic polarons or clusters with itinerant charges in either antiferromagnetic insulating matrix or paramagnetic insulating matrix or random mixtures of ferromagnetic metallic and antiferromagnetic insulating domains of various sizes. Some of the experimental evidences are: mobile ferromagnetic droplets in the antiferromagnetic  $\text{La}_{1-x}\text{Ca}_x\text{MnO}_3$  ( $x = 0.08, 0.1$ )<sup>1</sup>, few ten angstrom size ferromagnetic clusters in the paramagnetic insulating phase of  $\text{La}_{0.67}\text{Ca}_{0.33}\text{MnO}_3$  -type compounds<sup>2</sup> nanometer to micron size ferromagnetic clusters within the charge ordered matrix of  $\text{La}_{0.5\pm\delta}\text{Ca}_{0.5\pm\delta}\text{MnO}_3$ ,  $\text{Nd}_{0.5\pm\delta}\text{Sr}_{0.5\pm\delta}\text{MnO}_3$  and  $(\text{PrLa})_{0.7}\text{Ca}_{0.3}\text{MnO}_3$ <sup>3</sup>. Although some recent theoretical models<sup>4</sup> predict phase separation of a few angstrom size, micron size domains found experimentally appears to be connected with structural phase separation<sup>5</sup>.

Most of the existing reports are on hole-doped ( $\text{Mn}^{3+}$  rich or  $x \leq 0.5$ ) compounds<sup>1-3</sup>. An interesting type of phase separation occurs in the electron-doped  $\text{Ca}_{0.85}\text{Sm}_{0.15}\text{MnO}_3$ . It is paramagnetic and single phase with orthorhombic ( $Pnma$ ) structure at 300 K, but it phase separates into *two long range antiferromagnetic* phases, G- and C- types below 130 K and coexist with each other in orthorhombic ( $Pnma$ ) and monoclinic ( $P2_1/m$ ) structures respectively down to 5 K<sup>6</sup>. Interestingly, this particular composition of mixed antiferromagnet showed the highest magnetoresistance in the series  $\text{Ca}_{1-x}\text{Sm}_x\text{MnO}_3$ <sup>7</sup>. The origin of colossal magnetoresistance in this compound is not understood yet. In this communication we bring out anomalous magnetic field history dependent behavior of resistivity and magnetization in  $x = 0.15$  and contrast our results with lower doping ( $x$ ) levels. We also establish the magnetic phase diagram for the first time.

Four probe resistivity measurements in the temperature range from 300 K to 5 K up to the maximum field of  $H = 7$  T was done using Quantum Design Physical Property Measuring system. Magnetization up to  $H = 5$  T was done using Quantum Design SQUID magnetometer in the temperature range 300 K-5 K. Measurements were done in three methods: in the zero field cooled (ZFC) and field cooled (FC) modes, the sample was cooled from 300 K to 5 K rapidly (10 K/min) in absence of external magnetic fields and in presence of a known field ( $H$ ) respectively and the data were taken while warming (2 K/min) from 5 K. In the thermal cycling under magnetic field (TCUF) mode, the sample was subjected to a known field ( $H$ ) at 300 K and the data were collected while cooling down to 5 K and warming back to 300 K at a rate of 2 K/min.

Fig. 1(a) shows the phase diagram of  $\text{Ca}_{1-x}\text{Sm}_x\text{MnO}_3$  obtained from the low temperature magnetization (Fig. 1(b)) and resistivity data. The spontaneous magnetization,  $M(0\text{T})$ , obtained from the linear extrapolation of high field data to  $H = 0$  T and the high field magnetization,  $M(5\text{T})$  from Fig. 1(b) show similar trend with  $x$ : a rapid increase in between  $x = 0.05$  and  $x = 0.075$ , a maximum around  $x = 0.12$  and a reduced value at  $x = 0.15$ . Even though  $M(H)$  of  $x = 0.075$ - $0.12$  at low fields resembles a long range ferromagnet,  $M$  increases continuously without saturation at higher fields. The magnetization at  $H = 5$  T,  $M(5\text{T})$ , is far below the value  $M(F)$  for the fully aligned  $t_{2g}^3$  and  $e_g^1$  spins. This important observation lead us to suggest a heterogeneous magnetic state in  $\text{Ca}_{1-x}\text{Sm}_x\text{MnO}_3$  as illustrated by the schematic diagrams in Fig. 1(a). Region I ( $0 < x \leq 0.05$ ) is characterized by ferromagnetic (FM) clusters (black circles) embedded in a uniform G-type antiferromagnetic (G-AF) background (hatched region). These ferromagnetic clusters are created by the polarization of  $\text{Mn}^{4+}$  ( $t_{2g}^3$ ) spins around the doped  $\text{Mn}^{3+}$  ( $t_{2g}^3 e_g^1$ ) ions by double exchange interaction and doped charges ( $e_g$  electrons) are itinerant within these clusters. The onset of ferromagnetic order within these clusters sets in at  $T_C = 118 \pm 3$  K as determined from low field susceptibility measurements and scarcely varies with doping level  $x$ . As  $x$  increases, FM clusters size increase and they percolate in region II ( $0.05 < x < 0.13$ ) still in G-AF background.

Region III ( $0.13 \leq x \leq 0.15$ ) is dominated by C-type magnetic order but smaller G-AF and FM clusters coexist. These changes in magnetic properties are also reflected in electrical resistivity at 5 K ( $\rho(5\text{K})$ ) which decreases by 5 orders of magnitude from  $x = 0$  to  $x = 0.12$  and increases again as the antiferromagnetic order changes to C-type. The samples in regions II show metallic like resistivity ( $d\rho/dT > 0$ ) below 100 K due to the percolation of FM clusters. The composition of our primary interest is  $x = 0.15$  which shows C-AF ordering in monoclinic structure below  $T_{NC} = 112$  K and coexist with orthorhombic FM ( $T_C \approx 118$  K) G-phases ( $T_{NG} \approx 118$  K).

Fig. 2(a) shows the resistivity  $\rho(T)$  recorded under the TCUF mode. As T decreases from 300 K,  $\rho(T)$  initially decreases linearly with T down to 200 K, shows a minimum around  $T_p = 160$  K and increases again below this temperature as shown by the enlarged view in the inset. However, a rapid increase in  $\rho(T)$  occurs at still lower temperature,  $T_{NC} = 112$  K and changes by 4 orders of magnitude as T lowers to 5 K. The data taken during warming from 5 K bifurcate from the cooling curve and maintains higher resistivity values in the temperature range 70 K-125 K suggesting the first order nature of the transition. The rapid decrease in  $\rho(T)$  around 125 K while warming closely correlates with disappearance of the C-type AF magnetic order as found by neutron diffraction<sup>6</sup>. We find a large reduction in  $\rho(T)$  below 115 K for various values of H, but a metallic-like resistivity behavior ( $d\rho/dT > 0$ ) is seen only at  $H = 7$  T below 80 K. We measured  $\rho(T)$  at  $H = 6$  T also (not shown here for clarity) but  $d\rho/dT$  was found to be negative below 110 K.  $\rho(T)$  under different values of H show hysteresis of nearly same width as in  $H = 0$  T data. The increase in  $\rho(7\text{T})$  just below 102 K is possibly related to the shift of  $T_{NC}$  from 112 K for  $H = 0$  T to 102 K for  $H = 7$  T. On the high temperature side, the resistivity minimum at  $T_p$  is gradually suppressed with increasing H as shown in the inset.

The unexpected magnetic field history dependence of  $\rho(T)$  is shown in Fig. 2(b). The FC resistivity curves (dashed lines) recorded while warming from 5 K are similar to those ones in Fig. 2(a). However, the ZFC curves (thick lines) are distinctively different: they are

higher in resistivities than their FC counterparts and the curves under different H closely resemble the temperature dependence of  $\rho(0T)$  itself. It should be noted that while the field cooled  $\rho(7T)$  decrease continuously with temperature below 70 K, the decrease of zero field cooled  $\rho(7T)$  below 75 K is overwhelmed by a resistivity upturn below 35 K. The resistivity ratio  $\rho_{FC}/\rho_{ZFC}$  between zero field cooling and field cooling is as small as  $1.5 \times 10^{-4}$  at 10 K and 7 T. These differences are found only in samples close to  $x = 0.15$  ( $0.13 \leq x \leq 0.15$ ) but *not* in any other compositions for  $x \leq 0.12$  as shown in the inset of Fig. 2(b) for the insulating compound  $x = 0.025$ .

Motivated by the above unusual magnetotransport results and keeping in mind that magnetotransport in these materials are sensitive to the underlying magnetic order, we investigated the field and temperature dependence of the magnetization (M) in details as shown in Fig. 3(a) and 3(b) corresponding to Fig. 2(a) and 2(b) respectively. The maximum of M under 0.01 T at  $T_{NC} = 112$  K (see Fig. 3(a)) while field cooling signals the onset of simultaneous C-type antiferromagnetism and orthorhombic( $Pnma$ ) to monoclinic( $P2_1/m$ ) transformation. The phase fraction of monoclinic phase increases from 64 % at 110 K to 94 % at 10 K<sup>6</sup>. We find that M(T) curve while field heating deviates from the field cooling branch starting from 70 K for H = 5 T (90 K for H = 0.01 T), keeps a value lower than the field cooled ones, reaches a maximum at about 2 K above than while cooling and merges with the field cooling curve above 120 K. This trend in M(T) is also reflected in  $\rho(T)$  in Fig. 2(a) which shows higher value of  $\rho$  while warming than cooling. These hysteresis behaviors in  $\rho(T)$  and M(T) are the consequence of first order magneto-structural transition involving nucleation of high resistance, C-type antiferromagnetic monoclinic phase in low resistance, paramagnetic orthorhombic matrix while cooling and vice versa on heating from low temperature. In concurrence with the resistivity behavior in Fig. 2(b), a large difference between ZFC (symbols) and FC (thick lines) magnetization occurs below 120 K (see Fig. 3(b)) and the difference increases with increasing H and decreasing T. No difference between FC and ZFC magnetizations for  $H \geq 1$  T is found for  $x \leq 0.12$ .

Fig. 4 allows us to have further insight into the magnetic behavior observed above. Field cycling (0 T $\rightarrow$ 1T $\rightarrow$  -1T $\rightarrow$ 1T) data recorded at 10 K after zero field cooling (marked 1 T(ZFC)) shows a rapid increase in M for less than 20 Oe and reaches a maximum value of 0.136  $\mu_B$ . However, M increases by 25 % at 1 T when the sample is field cooled (marked as 1 T(FC)) from T  $>$ T<sub>NC</sub> (125 K). A large enhancement in M under field cooling is clearly seen for all the measured values of H and we do not find hysteresis in M up to 2 T. The right inset of Fig. 4 compares M cooled under 5 T to the zero field-cooled curve at 5 K. For H = 4 T (main panel) and 5 T (right inset), M has higher values while decreasing H from its maximum value H<sub>max</sub> to 0 T, but on subsequent field cycling (0 T $\rightarrow$  -H<sub>max</sub>  $\rightarrow$  +H<sub>max</sub>) M settles to slightly lower values. This behaviour is *not* caused by time dependent decay of magnetization since the data were recorded 5-10 minutes after the stabilization of temperature. M at H = 5 T (in the virgin field-cooled curve) is enhanced by a factor of with respect to zero field-cooled value at 5 T (M<sub>FC</sub>/M<sub>ZFC</sub> = 2.7). The observed enhancement of magnetization occurs *only* if the sample is field cooled from T  $>$ T<sub>N</sub> and not if T  $<$ T<sub>N</sub>. We find similar trends in 0.13  $\leq$  x  $\leq$  0.15 but do not observe in other compositions (x  $<$ 0.12) as shown for x = 0.025 in the left inset.

The surprising magnetic field history dependent properties found for x = 0.15 but not for x = 0.025 (or x  $\leq$  0.12) are difficult to understand from view point of magnetic heterogeneity alone because it prevails in both (and in all) these compounds. The increasing value of low field magnetic moments under field cooling for increasing strength of H suggests that more and more spins are getting aligned with H and the ferromagnetic clusters increase in size. It is unlikely that spins in the G-type AF phase contribute to this behavior because such trends lack for x  $\leq$  0.12. Since the enhancement of M is found *only* when the sample is field cooled from T  $>$ T<sub>N</sub> ( = T<sub>S</sub>, the transition temperature for structural transition), spins in the interfacial region between monoclinic C-type AF and orthorhombic FM phase might play important role. A pronounced increase in field cooled magnetization even at high values of H was first discovered for ferromagnetic nanoparticles of Co covered with antifer-

romagnetic CoO layers<sup>8</sup> and studied extensively in recent times in connection with exchange anisotropy/exchange biasing between ferromagnetic-antiferromagnetic films<sup>9,10</sup>. Field cooling Co/CoO mixtures from  $T > T_C$  ( where  $T_C$  is the ferromagnetic Curie temperature of Co) aligns magnetic moments of single domain Co particles in the field direction but certain fraction of spins of antiferromagnetic CoO at the interface are exchange coupled to Co moments which aligns themselves with Co spins. However, hysteresis loop of such exchange coupled systems made under FC mode are shifted from the origin which we do not see in our compounds. It does not mean that exchange coupling is not playing role in our compound. Existing theoretical model<sup>10,9</sup> assume that there are no macroscopic structural changes under external magnetic fields on either side of the interface. But, there are clear evidences that field induced structural changes accompany antiferro to ferromagnetic transition in manganites as we have shown for  $\text{Nd}_{0.5}\text{Sr}_{0.5}\text{MnO}_3$ .<sup>11,5</sup> This compound is also structurally and magnetically phase separated with minority long range ferromagnetic orthorhombic phase coexisting with majority charge ordered antiferromagnetic monoclinic phase at low temperatures and we also find magnetic history dependent behavior similar to  $\text{Ca}_{0.85}\text{Sm}_{0.15}\text{MnO}_3$  as shown in Fig. 5. Our neutron diffraction study under magnetic fields in  $\text{Ca}_{0.85}\text{Sm}_{0.15}\text{MnO}_3$ , although not done in a systematic way as done here, confirms monoclinic to orthorhombic transformation whose fraction also depends on the temperature and the strength of external magnetic field<sup>12</sup>.

In the absence of any theoretical models dealing with such exchange biasing relevant to manganites, we borrow our ideas from the random field model of Imry and Ma<sup>13</sup> which was applied to variety of different systems including exchange anisotropy/bias systems<sup>10</sup>, Ising antiferromagnets with random impurities<sup>14,15</sup>, mixed Ising Jahn-Teller system<sup>16</sup>  $\text{DyV}_{1-x}\text{As}_x\text{O}_4$  and martensitic transformation<sup>17</sup> and relaxor ferroelectrics<sup>18</sup>. The basic idea of Imry and Ma<sup>13</sup> is that systems in which random field effects dominates, domain formation is energetically favoured over long range order. Experimental realization of random field effect in an Ising antiferromagnet with random impurities is obtained under

field-cooled condition<sup>14,15</sup>.  $\text{Ca}_{0.85}\text{Sm}_{0.15}\text{MnO}_3$  with C-type antiferromagnet in which successive ferromagnetic linear chains along c-axis are coupled antiferromagnetically is an Ising antiferromagnet. The C-type antiferromagnetic phase also exhibits cooperative Jahn-Teller distortion due to ordering  $e_g$ - $d_{z^2}$  orbitals along c-axis<sup>6</sup>. The quenched random impurities are the G-type and FM phases. In zero field cooled measurement, the long range order corresponds to the coexistence of majority C-type AF phase and minority G-type AF phase and FM phases. The resistivity of zero field-cooled state is high as electron hopping between antiferromagnetically coupled  $\text{Mn}^{3+}$  and  $\text{Mn}^{4+}$  sites is not favoured by double exchange interaction. Field cooling enhances the size of ferromagnetic regions and, breaks the C-type AF matrix into domains due to random field effect<sup>13-15</sup>. Then, domain walls in which spins are not exactly antiparallel along with the expanded FM regions in the orthorhombic phase constitute least resistance path for electrical conduction and resistivity decreases. As the external field increases above 4 T, a partial structural transformation from monoclinic, C-type antiferromagnetic to orthorhombic (ferromagnetic) also takes place. Our neutron diffraction results<sup>12</sup> suggest that a complete monoclinic to orthorhombic structural transformation occurs at  $T = 100$  K and  $H = 6$  T but the transformation is only partial at low temperatures (60 % monoclinic and 40 % orthorhombic at 40 K and  $H = 6$  T after a zero field cooled process). Hence, when the sample is field cooled for  $H \geq 4$  T, the magnetic moment is initially high (see the inset of Fig. 4) since the orthorhombic ferromagnetic phase contributes largely to the observed magnetization but its fraction decreases as  $H$  is reduced to zero. Upon further field cycling from  $0 \text{ T} \rightarrow -5T \rightarrow 5T$  magnetization locks to a value determined by the new phase fraction of orthorhombic/monoclinic phases. Thus, the field cooling is more efficient in reducing the resistivity than the zero field cooling. The absence of Ising spin character and structural variants in lower doped compounds is the most likely the reasons why we fail to observe magnetic field history dependent behaviors for lower  $x$ .

In conclusion, resistivity and magnetization of the electron doped compound  $\text{Ca}_{0.85}\text{Sm}_{0.15}\text{MnO}_3$  reveals first order nature of paramagnetic-antiferromagnetic transition and



field cooling enhances magnetization, reduces resistivity and even induces insulator-metal transition for  $H = 7$  T whereas it is an antiferromagnetic insulator when cooled in zero field. No difference between field cooled and zero field cooled resistivities are found for  $x \leq 0.12$ . These differences are suggested to the mixed phase (two antiferromagnetic phases and a ferromagnetic phase coexisting in two different crystallographic structures) nature of  $\text{Ca}_{0.85}\text{Sm}_{0.15}\text{MnO}_3$  in zero field and formation of AF domain states and structural transition under magnetic fields.

R.M thanks MNERT (France) for financial support and acknowledges discussions with Professors T. V. Ramakrishnan, M. R. Ibarra, D. I. Khomskii and Drs. Venkatesh Pai, C. Ritter and P. A. Alagarebel.

## REFERENCES

- <sup>1</sup> M. Hennion, F. Moussa, J. Rodriguez-Carvajal, L. Pinsard, and A. Revcolevschi, *Phys. Rev. B* **56**, R497 (1997).
- <sup>2</sup> J. M. de Teresa, M. R. Ibarra, C. Marquina, P. A. Algarabel, C. Ritter, J. Garcia, J. Blasco, A. del Morel, and Z. Arnold, *Nature* **386**, 256 (1997); J. Z. Sun, L. Krusin-Elbaum, A. Gupta, and G. Xiao, *Appl. Phys. Lett.* **69**, 1002 (1996).
- <sup>3</sup> S. Mori, C. H. Chen, and S. W. Cheong, *Phys. Rev. Lett.* **81** 3972 (1998); R. Mahendiran, M. R. Ibarra, A. Maignan, A. Arulraj, R. Mahesh, B. Raveau, and C. N. R. Rao, *Phys. Rev. Lett.* **82**, 2191 (1999); R. Mahendiran, M. R. Ibarra, A. Maignan, C. Martin, B. Raveau, and A. Hernando, *Solid State Commun.* **111**, 525 (1999); G. Allodi, F. Licci, and W. Pepper, *Phys. Rev. Lett.* **81** 4736 (1999); M. Roy, P. Schiffer, and A. P. Ramirez, *Phys. Rev. B* **58**, 5158 (1999); M. R. Ibarra, G. M. Zhao, J. M. de Teresa, Z. Arnold, C. Marquina, P. A. Algarabel, H. Keller, and C. Ritter, *Phys. Rev. B* **57**, 7446 (1998); N. Babuskina, L. M. Belova, D. I. Khomskii, K. I. Kugel, O. Yu. Gorbekko, and A. R. Kaul, *Phys. Rev. B* **59**, 6994 (1996).
- <sup>4</sup> E. L. Nagaev, *Physics Uspekhi* **39**, 781 (1996); A. Moreo, S. Yunoki, E. Dagoto, *Science*, **283**, 2034 (1999); M. Yu. Kagan and D. I. Khomskii, *Euro. Phys. J. B* **12**, 217-223 (1999); L.P. Gork'ov and V. Z. Kresin, *JETP Lett.* **67**, 985 (1998)
- <sup>5</sup> C. Ritter, R. Mahendiran, M. R. Ibarra, A. Maignan, B. Raveau, and C. N. R. Rao, *Phys. Rev. B* **61**, R9229 (2000).
- <sup>6</sup> C. Martin, A. Maignan, M. Hervieu, B. Raveau, Z. Jirak A. Kurbakov, V. Tronouv, G. Andre, and F. Bouree, *J. Magn. Magn. Mater.* **205**, 184 (1999).
- <sup>7</sup> C. Martin, A. Maignan, F. Damay, M. Hervieu, and B. Raveau, *J. Solid State Chem.* **134**, 198 (1997).
- <sup>8</sup> W. H. Meiklejohn and C. P. Bean, *Phys. Rev.* **102**, 1413 (1956).

- <sup>9</sup> For review see, A. E. Berkowitz and K. Takano, *J. Magn. Magn. Mater.* **200**, 552 (1999)
- <sup>10</sup> A. P. Malozemoff, *J. Appl. Phys.* **63**, 3874 (1988).
- <sup>11</sup> R. Mahendiran, M. R. Ibarra, A. Maignan, F. Millange, A. Arulraj, R. Mahesh , B. Raveau, and C. N. R Rao, *Phys. Rev. Lett.* **82**, 2191 (1999).
- <sup>12</sup> R. Mahendiran, M. R. Ibarra, P. A. Algarebel, A. Maignan, C. Martin, B. Raveau, and C. Ritter (unpublished).
- <sup>13</sup> Y. Imry and S. Ma, *Phys. Rev. Lett.* **35**, 1399 (1975).
- <sup>14</sup> G. S. Grest, C. M. Soukoulis, and K. Levin, *Phys. Rev.* **B 33**, 7659 (1986).
- <sup>15</sup> For review see, D. P. Belanger in *Spin glass and Random fields*, World Scientific (Singapore 1997).
- <sup>16</sup> J. T. Graham, M. Maliapaard, J. H. Page, S. R. P. Smith, and D. R. Taylor, *Phys. Rev.* **B 35**, R2098 (1987).
- <sup>17</sup> S. Semenovskaya and A. G. Khachuryan, *J. Appl. Phys.* **83**, 5125 (1998).
- <sup>18</sup> V. Westphal, W. Kleemann, and M. D. Glinchuk, *Phys. Rev. Lett.* **68**, 847 (1992).

## FIGURE CAPTIONS

**Fig.1** : (a). Phase diagram of  $\text{Ca}_{1-x}\text{Sm}_x\text{MnO}_3$  ( $0 \leq x \leq 0.15$ ).  $\rho(5\text{K})$ : Resistivity at 5 K,  $M(5\text{ T})$ : Magnetization at  $H = 5\text{ T}$  and at 5 K.  $M(0\text{T})$ : Extrapolation of high field  $M$  to  $H = 0\text{ T}$ .  $M(\text{F})$ : Expected magnetic moments for fully ferromagnetically aligned  $t_{2g}$ ,  $e_g$  spins. Lines are guide to the eyes. Black circle: Ferromagnetic clusters, Hatched regions: G- and C- type antiferromagnetic phases. (b). Field dependence of magnetization at 5 K for  $\text{Ca}_{1-x}\text{Sm}_x\text{MnO}_3$ .

**Fig.2** :(a). Resistivity ( $\rho$ ) of  $x = 0.15$  recorded during thermal cycling under magnetic field (TCUF). Arrows indicate the direction temperature sweep. Inset: expanded view of  $\rho$  above 100 K. (b).  $\rho(T)$  made under zero field-cooled (thick lines) and field-cooled (dashed lines). Inset:  $\rho(T)$  of  $x = 0.025$ . Double head arrows are to indicate perfect reversibility. Note that there is no difference in  $\rho(T)$  between zero field cooling and field cooling conditions.

**Fig.3** : (a). Magnetization ( $M$ ) of  $x = 0.15$  made under the TCUF mode. (b).  $M$  under ZFC (symbols connected by lines), FC (thick lines) modes.

**Fig.4** : Main panel: Magnetic field cycling of magnetization made under field cooled (FC) mode ( $+H_{max} \rightarrow -H_{max} \rightarrow +H_{max}$ ) for  $H_{max} = 1\text{ T}, 2\text{ T}, 3\text{ T}, 4\text{ T}$ . Magnetization under zero field cooled (ZFC) mode ( $0\text{ T} \rightarrow +H_{max} \rightarrow -H_{max} \rightarrow +H_{max}$ ) is also shown for 1 T. Double head arrows are to indicate the complete reversibility. Right inset :  $M$  under ZFC and FC modes up to  $H = 5\text{ T}$ . Left inset:  $M$  of  $x = 0.025$ . Note that there is no difference in  $M$  between FC and ZFC mode.

**Fig.5** : Resistivity of  $\text{Nd}_{0.5}\text{Sr}_{0.5}\text{MnO}_3$  made under zero field-cooled (thick lines) and field-cooled (dashed lines) modes. Arrows indicate the direction of temperature sweep.

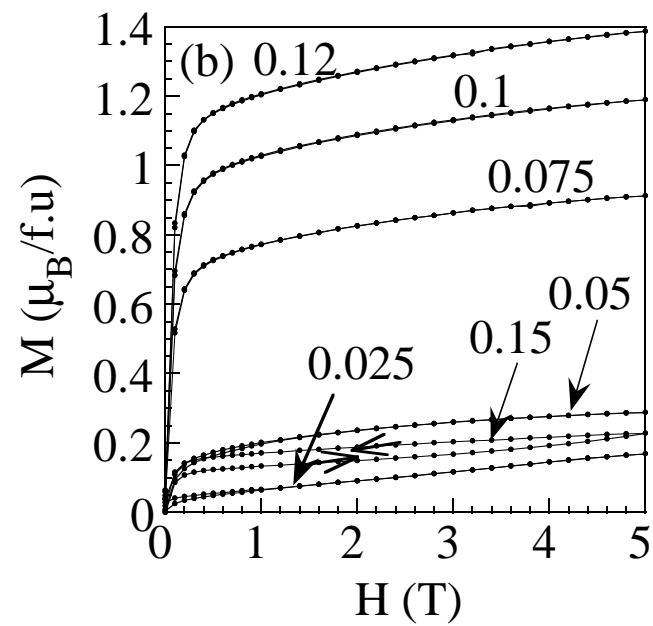
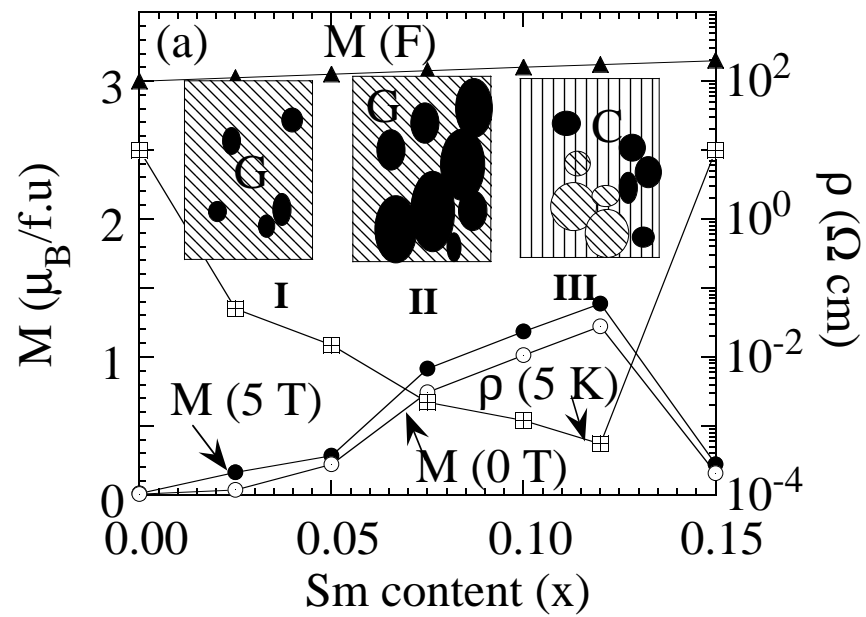


FIG. 1 (two column)  
R. Mahendiran et al

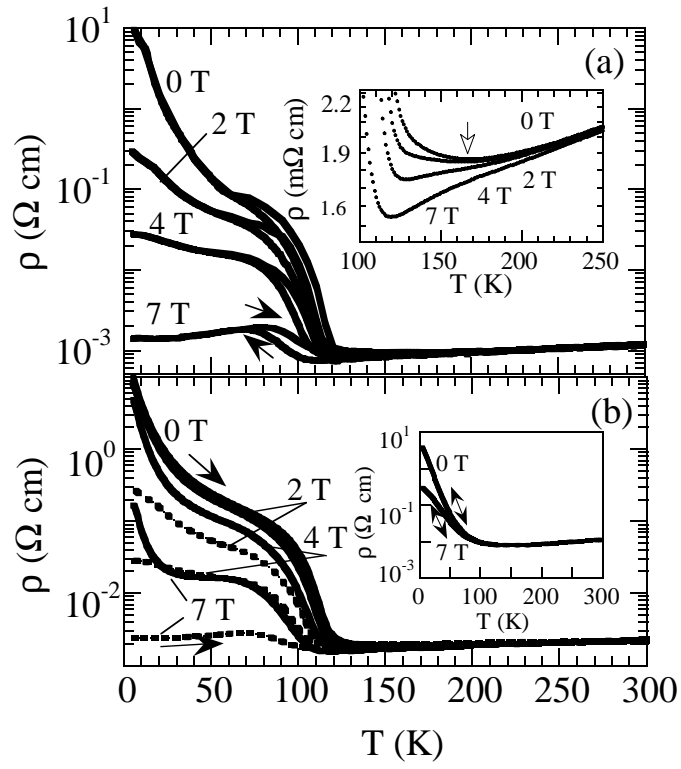


FIG.2  
R. Mahendiran et al

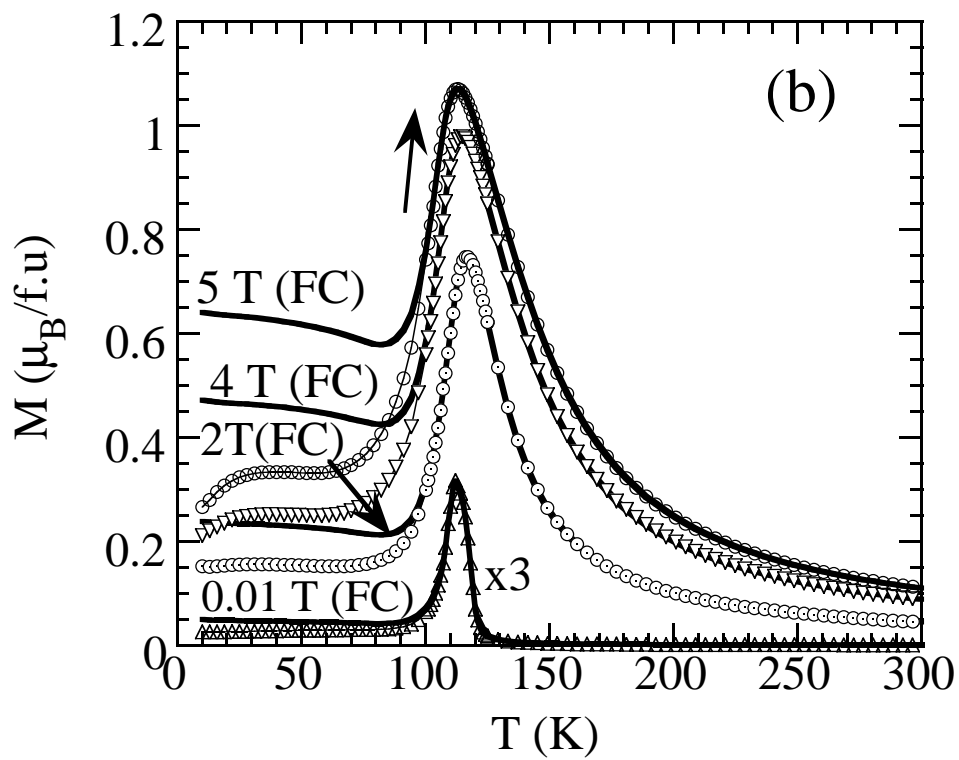
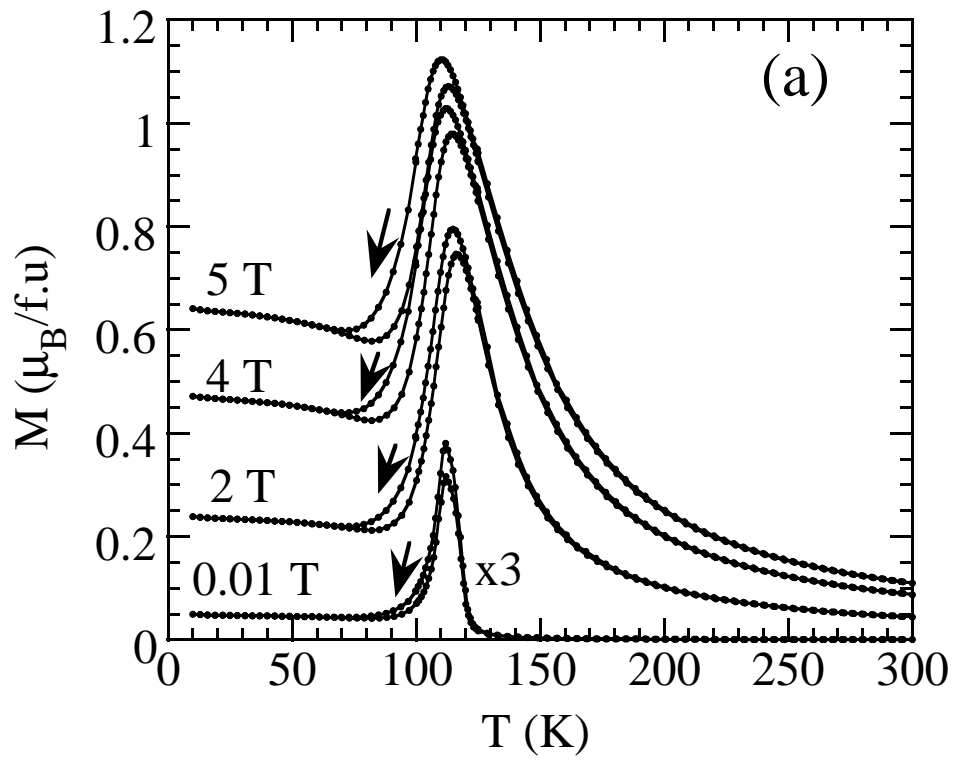


FIG. 3  
R. Mahendiran et al

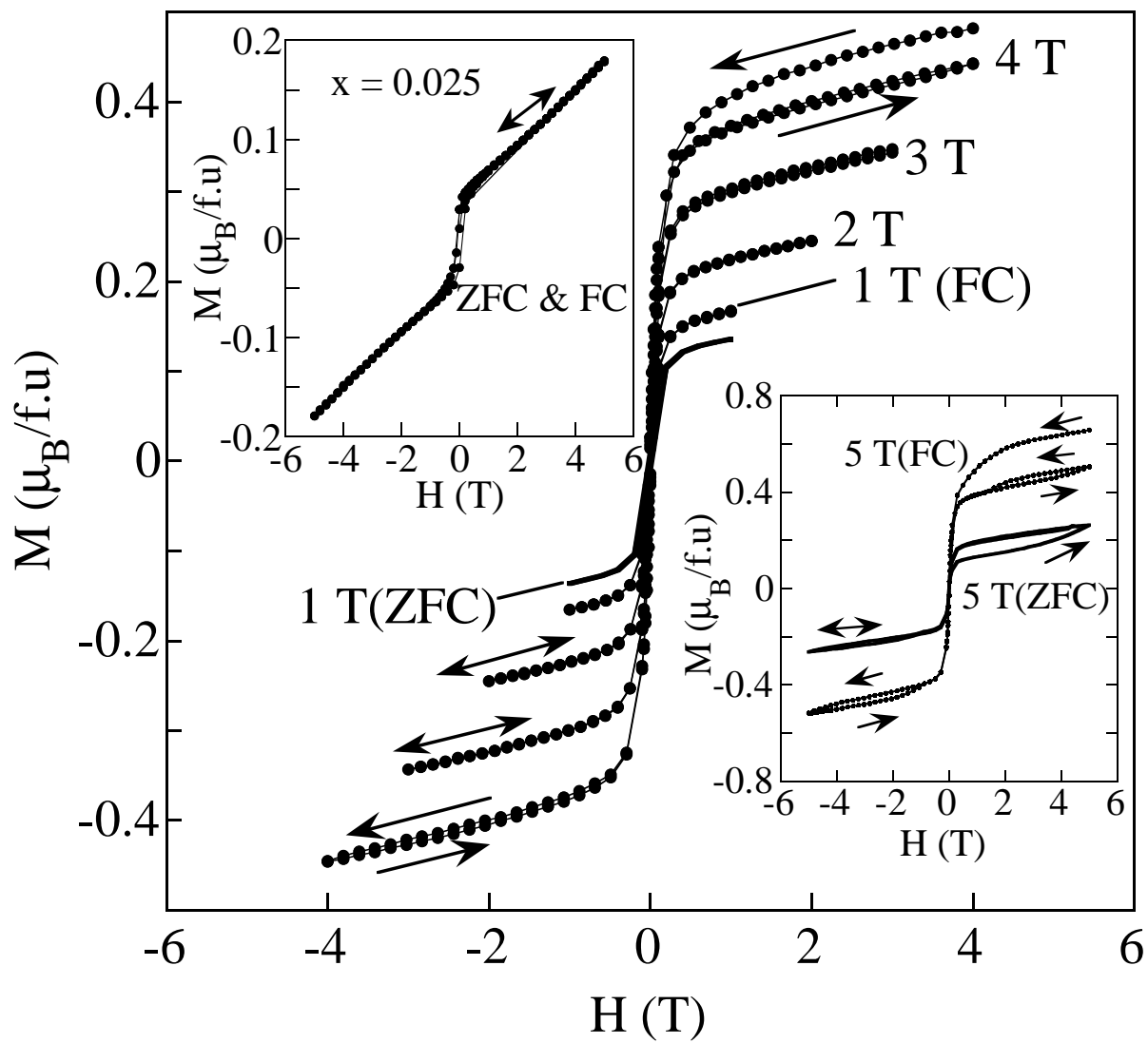


FIG. 4  
 R. Mahendiran et al



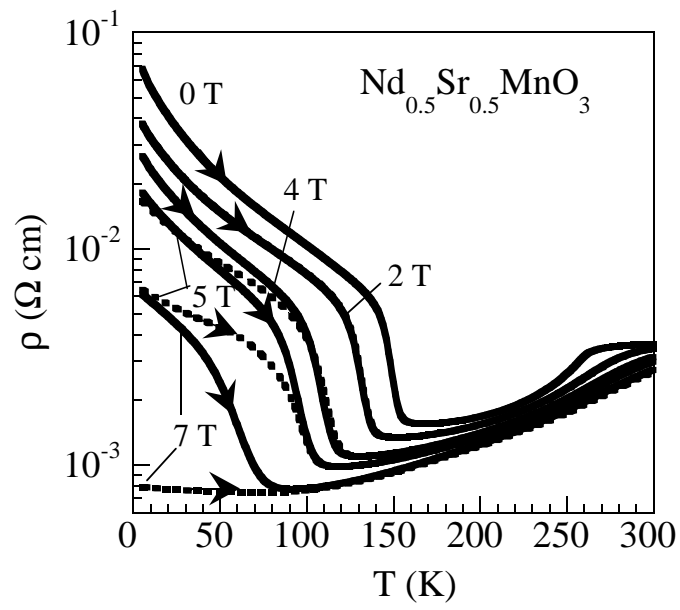


FIG.5  
R. Mahendiran et al